NAVAL POSTGRADUATE SCHOOL
MONTEREY, CALIFORNIA

THESIS

WAVE SLOPES AND BREAKING DISTRIBUTIONS IN THE SURF ZONE

by

Carther Frederic Jorgensen

March, 1996

Thesis Advisor:	Edward B. Thornton
Co-Advisor:	Thomas C. Lippmann

Approved for public release; distribution is unlimited.

REPORT DOCUMENTATION PAGE

Form Approved OMB No. 0704-0188

1. AGENCY USE ONLY *(Leave blank)*	2. REPORT DATE	3. REPORT TYPE AND DATES COVERED
	March, 1996.	Master's Thesis

4. TITLE AND SUBTITLE WAVE SLOPES AND BREAKING DISTRIBUTIONS IN THE SURF ZONE

5. FUNDING NUMBERS

6. AUTHOR(S) Carther Frederic Jorgensen

7. PERFORMING ORGANIZATION NAME(S) AND ADDRESS(ES)
Naval Postgraduate School
Monterey CA 93943-5000

8. PERFORMING ORGANIZATION REPORT NUMBER

9. SPONSORING/MONITORING AGENCY NAME(S) AND ADDRESS(ES)

10. SPONSORING/MONITORING AGENCY REPORT NUMBER

11. SUPPLEMENTARY NOTES The views expressed in this thesis are those of the author and do not reflect the official policy or position of the Department of Defense or the U.S. Government.

12a. DISTRIBUTION/AVAILABILITY STATEMENT
Approved for public release; distribution is unlimited.

12b. DISTRIBUTION CODE

13. ABSTRACT (maximum 200 words)

Field measurements from a cross-shore array of nine pressure sensors, spanning the surf zone, are used to examine the evolution of ensemble averaged wave face slopes of ocean waves as they propagate through the breaking region. Averaged wave slopes are determined from time series of the measured sea surface elevation and from an averaged waveform calculated from bispectral coefficients, and compared with predictions from a wave transformation model that includes wave breaking described by rollers. Measured percent wave breaking are used to examine the evolution of third moment and bispectral statistics in relation to breaking patterns.

Shoaling waves gradually transform from peaked, Stokes-like waves to forward pitched asymmetric waves just prior to breaking. Inside the surf zone, wave asymmetry is modified by the breaking distributions and the effects of bottom topography. The observations suggest a relationship between the cross-shore wave breaking distributions and wave slopes. Wave slopes predicted using a calibrated wave transformation model which includes wave rollers are in qualitative agreement with measured wave slopes.

14. SUBJECT TERMS Delilah, Breaking, Waves, Slopes, Asymmetry, Skewness, Bispectral, Biphase, Bicoherence, Roller	15. NUMBER OF PAGES 64
	16. PRICE CODE

17. SECURITY CLASSIFICATION OF REPORT	18. SECURITY CLASSIFICATION OF THIS PAGE	19. SECURITY CLASSIFICATION OF ABSTRACT	20. LIMITATION OF ABSTRACT
Unclassified	Unclassified	Unclassified	UL

NSN 7540-01-280-5500

Standard Form 298 (Rev. 2-89)
Prescribed by ANSI Std. 239-18 298-102

Approved for public release; distribution is unlimited

WAVE SLOPES AND BREAKING DISTRIBUTIONS IN THE SURF ZONE

Carther F. Jorgensen
Lieutenant, United States Navy
B.S., United States Naval Academy, 1989

Submitted in partial fulfillment
of the requirements for the degree of

MASTER OF SCIENCE IN (PHYSICAL OCEANOGRAPHY)

from the

NAVAL POSTGRADUATE SCHOOL
March 1996

Author: Carther F. Jorgensen
Carther F. Jorgensen

Approved by: Edward B. Thornton
E. B. Thornton, Thesis Advisor

Thomas C. Lippmann
T. C. Lippmann, Co-Advisor

Robert H. Bourke
R. H. Bourke, Chairman
Department of Oceanography

ABSTRACT

Field measurements from a cross-shore array of nine pressure sensors, spanning the surf zone, are used to examine the evolution of ensemble averaged wave face slopes of ocean waves as they propagate through the breaking region. Averaged wave slopes are determined from time series of the measured sea surface elevation and from an averaged waveform calculated from bispectral coefficients, and compared with predictions from a wave transformation model that includes wave breaking described by rollers. Measured percent wave breaking are used to examine the evolution of third moment and bispectral statistics in relation to breaking patterns.

Shoaling waves gradually transform from peaked, Stokes-like waves to forward pitched asymmetric waves just prior to breaking. Inside the surf zone, wave asymmetry is modified by the breaking distributions and the effects of bottom topography. The observations suggest a relationship between the cross-shore wave breaking distributions and wave slopes. Wave slopes predicted using a calibrated wave transformation model which includes wave rollers are in qualitative agreement with measured wave slopes.

TABLE OF CONTENTS

LIST OF SYMBOLS

a = amplitude function

a_o = amplitude of primary frequency

A = Fourier transform

A = wave roller

A = area per unit crest length of turbulence

b = Bicoherence

B = bispectrum

B = horizontal fraction of wave face covered by roller

β = Bicoherence

c = wave phase speed

c_g = wave group velocity

d = derivative

e = exponent

E = expected value

E_r = energy in wave roller

E_w = energy in wave motion

e = wave pitch

f = frequency (hz)

f_o = incident frequency (hz)

f_p = peak frequency (hz)

$\mathcal{F}$ = Fourier transform

h = water depth

h_o = water depth at breaking

H = wave height

H = Hilbert transform

H_b = breaking wave height

H_o = incident wave height

H_{rms} = significant wave height

$\mathscr{H}$ = Hilbert transform

i = imaginary part

$\Im$ = imaginary component

L = local wave length

L_j = horizontal length of wave jump

L_r = horizontal length of wave roller

n = number

η = sea surface elevation

ω = radian frequency

ω_o = radian frequency of first harmonic

P = power spectrum

ϕ = biphase

ψ = spatially invariant wave slope tuning parameter

π = 3.14

$\Re$ = real component

σ = slope at wave / roller interface

σ = angle of jump discontinuity

t = time

τ = time lag

τ_s = shear stress at wave roller interface

θ = phase relative to primary frequency

ξ = time series

u = function of time

x = cross-shore distance

$\langle\ \rangle$ = ensemble averaging

ACKNOWLEDGMENTS

This research was funded by the Office of Naval Research, Coastal Sciences Program under contract #N00114-95-AF-0002. Excellent logistic support for the Delilah experiment were provided by the staff of the U. S. Army Corps of Engineers, Coastal Engineering Research Center (CERC) Field Research Facility (FRF) at Duck, North Carolina under the direction of Bill Birkemeier. Video data were collected and graciously provided by Rob Holman of Oregon State University. The pressure sensors and data collection system were developed and maintained by Tim Stanton and Rob Wyland of the Naval Postgraduate School. The work benefited from the insightful suggestions by Tom Herbers and Bob Guza.

I. INTRODUCTION

As waves shoal in intermediate water depths, nonlinear interactions transfer incident wave energy from the peak incident frequency to both higher (harmonics) and lower (infragravity) frequencies. The strength of these interactions depend on many factors, which include incident wave properties, topography and whether or not breaking is occurring. On the inner shelf, wave energy flux is approximately conserved. However, in very shallow water, shoaling waves become unstable and eventually break (creating the surf zone), and organized wave energy is converted to turbulence and dissipated. Turbulence generated in the surface boundary layer by wave breaking is the primary dissipative mechanism in the surf zone. To model wave transformation all the way to the shoreline requires that the dissipative mechanism be specified.

A common approach to describing breaking wave dissipation has been to use the analogy of a hydraulic jump to bores in the surf zone (LeMehaute, 1962; Engelund, 1981). This approach has been successful at predicting wave transformation across arbitrary bathymetry (e.g., Battjes and Janssen, 1978; Thornton and Guza, 1983; Roelvink, 1993; Lippmann, *et al.*, 1996). Many of these models use empirical weighting functions to describe the portion of wave breaking. Although they do a good job of predicting wave

heights, the spatial distribution of wave breaking is not always well represented. An improvement to the wave transformation model using the concept of wave rollers (as described in Duncan, 1981; Engelund, 1981; Svendsen, 1984; and others) has resulted in a better representation of breaking distributions, as shown in Figure 1 by comparing the roller model by Lippmann and Thornton (1996), henceforth referred to as LT96, (solid line) with a typical wave transformation model (dashed line). The formulation of wave breaking in roller models (Svendsen, 1984; Nairn, *et al.*, 1990; Dally and Brown, 1995; LT96; and others) suggests that the slope of the front face of the wave is important in determining the spatial variation in wave breaking distributions in the surf zone.

These models incorporate roller energy advection terms in an energy balance equation that retains the energy flux within a turbulent mass of water perched on the wave face (the roller) as waves break, advects roller energy landward, and then loses energy to turbulent dissipation in the underlying water column by action of the shear stresses at the wave/roller interface. The energy flux balance is described by

$$\frac{\partial E_w C_g}{\partial x} + \frac{\partial E_r C}{\partial x} = -\tau_s C \qquad (1)$$

where E_w and E_r are wave and roller energy, C_g is the group

velocity, C is phase speed of shallow water waves, and τ_s is the shear stress at the wave/roller interface. Both the roller energy and shear stress depend on the roller area, A (Duncan, 1981; Svendsen, 1984; Deigaard, 1993; and others). The size of A is determined from the energy lost in a hydraulic jump of height, H. The area is determined by the energy lost to turbulence while conserving mass and momentum both upstream and downstream of the flow discontinuity (Engelund, 1981). The area per unit crest length of the roller describing the turbulence generated in the jump is given by

$$A = \frac{H^3}{4h\tan\sigma} \tag{2}$$

where h is the water depth and σ is the angle of jump discontinuity. The spatial variation of the rollers thus depends on σ. A schematic showing the geometry of a wave with a turbulent roller on a linear wave face is depicted in Figure 2. Using simple geometrical approximations (Figure 2), σ is given by a function of breaking wave steepness (H_b/L)

$$\langle\tan\sigma\rangle = \langle\frac{H_b}{L}\rangle \psi \tag{3}$$

where $\langle\ \rangle$ indicates ensemble averaging, L is the local wavelength, and ψ (which is equivalent to B/e where B and e

are the fractions of wave height and wave length covered by the roller) is an assumed spatially invariant constant dependent on how skewed or pitched forward the waveform.

The value of ψ is a free parameter and used as a calibrating constant to give a best fit to the observations of concurrent sea surface elevation and wave breaking statistics (obtained by pressure sensors and video recordings of the surf zone). The wave data is used to estimate how well Equation 3 resembles the actual breaking wave slopes.

The objective of this paper is to examine evolution of the wave face slope across the breaking region and compare the observations with the LT96 roller model predictions to assess the formulation of the model. Two methods, time series and bispectral, are used to calculate wave slopes from pressure sensor data. Slopes calculated directly from the time series include contributions by all incident waves. In the bispectral method, a slope is calculated from a single averaged waveform composed of a primary wave and its nonlinearly coupled harmonics whose amplitudes and phases are determined from the bispectrum. The roller model predicted wave face slopes are compared to both the average slopes calculated from time series and bispectral methods.

The next section describes how statistics from pressure sensors are used to calculate wave face slopes. In the experiment section, the field measurements of sea surface

elevation and wave breaking obtained during the 1990 Delilah experiment are described. In the results and discussion, the evolution of the qualitative behavior of wave nonlinearities are examined as waves propagate shoreward through the surf zone. Observations of percent wave breaking, nonlinear third moments (skewness and asymmetry), and bispectral statistics are examined in relationship to bathymetry. The cross-shore behavior of ensemble averaged wave slopes is compared with predictions from the LT96 roller model calibrated with observations of wave breaking.

II. ANALYSIS

As waves shoal in intermediate water depth, they become Stokes-like with peaked crests and lengthened, shallow troughs. As waves enter progressively shallower depths, they begin to pitch forward until they break creating the surf zone. Across the shoaling and breaking regions, energy at the primary frequencies is transferred nonlinearly to both lower and higher frequencies. The higher frequency forced waves are phase-coupled to the primary. The degree of coupling and phase relationship between primary and harmonic frequencies result in wave deformation leading to breaking and are quantified with higher (third) order spectral techniques (the bispectrum).

The waveform evolution of shoaling surface gravity waves is described using the third moment wave statistics, skewness and asymmetry, of the time series (Elgar and Guza, 1985). Profiles for both skewed and asymmetric waveforms are shown in Figure 3 (taken with slight modification from Doering, 1988). Skewed waves are similar to Stokes waves, characterized by a peaked wave profile with elongated and flattened troughs, and a lack of symmetry about the horizontal axis. Asymmetric waves resemble a pitched forward profile like "saw-tooth" bores common to the surf zone. Both skewed and asymmetric waves have the same amplitude spectrum as illustrated by the Fourier decomposition in

Figure 3. The phase shifting of harmonic components relative to the primary frequency is a characteristic of asymmetric and skewed waves. The difference is in the phase spectrum, also shown in Figure 3. The skewed waves have phase-locked harmonics in-phase with the primary frequency. A purely asymmetric waveform, or saw-toothed profile, has the n^{th} harmonic phase shifted $\pi/2$ relative to the primary frequency. All other phase relationships result in waves having both skewed and asymmetric characteristics.

First order spectral techniques cannot be used to fully examine these higher order moments. Higher order spectra (bispectrum) have been applied to ocean surface gravity waves to study nonlinear phenomena for several decades (Hasselman, *et al.*, 1963, and others). Elgar and Guza (1985) calculated bispectra of shoaling waves and found that harmonic growth and biphase evolution across the shoaling region was consistent with gross changes in wave shape, and used this technique to study the evolution of both skewness and asymmetry in the shoaling region.

If we represent waves entering the surf zone by a stationary Gaussian function of time with zero mean, $\xi(t)$, then the wave field is represented by a superposition of statistically independent wave components. Thus, the time series is completely described by the double-sided energy-density spectrum, S(f), expressed in terms of Fourier coefficients, $\mathcal{F}(f)$,

$$S(f) = E[\mathcal{F}(f)\ \mathcal{F}^*(f)] \ / \ \Delta f \qquad (4)$$

where f is frequency, Δf is the frequency bandwidth, and E[] is the expected value operator. The variance of the time series is simply the integral of the energy-density spectrum

$$E[\xi^2(t)] = \int_{-\infty}^{\infty} S(f)df \qquad (5)$$

The bispectrum can also be expressed in terms of Fourier coefficients (Hasselmann, *et al., 1963*; Kim and Powers, 1979)

$$B(f_1,f_2) = E[\mathcal{F}(f_1)\ \mathcal{F}(f_2)\ \mathcal{F}^*(f_1+f_2)] \ / \ \Delta f^2 \qquad (6)$$

The bispectrum is nonzero only if waves at frequencies f_1 and f_2 are nonlinearly coupled, generating both sum and difference frequencies, f_3,

$$f_1 \pm f_2 = f_3 \qquad (7)$$

Unlike the energy-density spectrum which is real only, the bispectrum is complex, having real and imaginary components which are related to third moment statistics.

The integral of the imaginary part ($\Im[\,]$) of the bispectrum normalized by the time series variance to the 3/2 power, is used to define the asymmetry

$$Asymmetry = \frac{\int_{-\infty}^{\infty}\int_{-\infty}^{\infty} \Im[B(f_1,f_2)]df_1df_2}{E[\xi^2(t)]^{3/2}} \qquad (8)$$

equivalent to the skewness of the Hilbert Transform (see Bendat and Piersol, 1986) of the time series (Elgar and Guza, 1985). Similarly, the normalized integral of the real part ($\Re[\,]$) of the bispectrum is used to define the skewness

$$Skewness = \frac{\int_{-\infty}^{\infty}\int_{-\infty}^{\infty} \Re[B(f_1,f_2)]df_1df_2}{E[\xi^2(t)]^{3/2}} \qquad (9)$$

equivalent to the third moment of the time series.

Bicoherence, b, is the normalized form of the bispectrum ($0 \le b \le 1$) and is used to separate independent, free waves from the nonlinearly phase-coupled waves (Kim and Powers, 1979)

$$b^2(f_1,f_2) = \frac{|B(f_1,f_2)|^2}{E[|\mathcal{F}(f_1)\ \mathcal{F}(f_2)|^2]\ E[|\mathcal{F}(f_1+f_2)|^2]} \qquad (10)$$

Values of bicoherence greater than the significance level for a given confidence interval indicates the presence of nonlinear coupling between interacting frequencies. The significance level for 95% confidence on nonzero bicoherence, b_{95}, is calculated as

$$b_{95}^2 = \frac{6}{dof} \tag{11}$$

where dof is the number of degrees of freedom (Elgar and Guza, 1985).

The biphase represents the relative phase relationship between the interacting frequencies and is determined by

$$\beta(f_1, f_2) = \tan^{-1}\left\{\frac{\Im[B(f_1, f_2)]}{\Re[B(f_1, f_2)]}\right\} \tag{12}$$

For significant bicoherent coupling at (f_1, f_2), biphase values of 0 represent contributions to a more skewed waveform (Figure 3), whereas values of -90° make the waveform more asymmetric (Figure 3). Other values of biphase indicate harmonics are contributing to both skewed and asymmetric waveforms.

Surface elevation slopes, $\partial\eta/\partial x$, are estimated from the time series of the sea surface elevation, $\eta(t)$, by

$$\frac{\partial \eta}{\partial x} = \frac{1}{c}\frac{\partial \eta}{\partial t} \qquad (13)$$

where x is cross-shore coordinate and t is time, and assuming that the wave field is non-dispersive with phase speeds dependent only on the (known) local depth, $c = \sqrt{gh}$ with g gravity. The differentiated surface elevation time series, $\partial\eta/\partial t$, is obtained in the frequency domain by applying the transfer function of $-i\omega$ to the complex Fourier amplitudes of $\eta(t)$ and inverse transforming back to the time domain. The surface slope is calculated as the maximum wave face slope found from the extrema of $\partial^2\eta/\partial t^2$. The second derivative of the surface elevation time series is obtained by applying the transfer function, $i^2\omega^2$, to the complex Fourier amplitudes of $\eta(t)$ and inverse transforming. The up-crossings are identified and the maximum positive slopes between the up-crossings are the slopes of the wave face. The ensemble averaged wave face slope is calculated as the rms slope.

As a second technique, the wave face slope is estimated from the averaged waveform represented as a primary wave at the peak incident frequency plus the nonlinearly coupled harmonics found from the bispectrum,

$$(t) = a_0\cos(\omega_0 t) + a_1 b_1\cos(2\omega_0 t - \phi_1) + a_2 b_2\cos(3\omega_0 t - \phi_2) + \ldots (14)$$

The time series represented by Equation 14 is periodic with frequency f_o. Phase locking makes all the waves appear to be the same. The same procedure for calculating the wave slopes used in the time series analysis is applied to Equation 14 over a single wave period. Thus, the maximum $\partial\eta/\partial x$ over one wave period defines the average angle of the wave face. The wave slope is now a function of a primary (a_o) and its coupled harmonic (a_1, a_2, ...) amplitudes, coupling coefficients or bicoherences (b_1, b_2, ...), and biphases (ϕ_1, ϕ_2,...).

III. FIELD EXPERIMENT

The data were collected as part of the Delilah Nearshore Processes experiment held at the U. S. Army Corps of Engineers Coastal Engineering Research Center Field Research Facility (FRF) in Duck, North Carolina during October 1990. Nine pressure sensors were deployed in a cross-shore array from ~4.5m depth to the shoreline (Figure 4). Data were acquired approximately continuously at 8 Hz for about 3 weeks.

Bottom pressure measurements were converted to sea surface elevation by Fourier transforming the one hour pressure record, applying the linear wave theory spectral transformation function, and inverse transforming to obtain sea surface elevation (Guza and Thornton, 1980). At the same time, the data were band-pass filtered from 0.05 to 0.5 Hz by zeroing the Fourier coefficients prior to inverse transforming to remove high frequency noise and lower frequency (infragravity) waves. The sea surface elevations were detrended, and subsampled to 2 Hz for subsequent analysis.

Video recordings of the surf zone were obtained from cameras mounted on a 44m high observation tower. The cross-shore distribution of the number of waves breaking at a particular location were estimated using the video taken during daylight hours. The number of waves breaking were

counted manually from video pixel time series (Lippmann and Holman, 1991) at approximately 10m intervals spanning the width of the surf zone.

The bottom profile was surveyed daily using the Coastal Research Amphibious Buggy (CRAB; Birkemeier and Mason, 1984). The bathymetry evolved significantly during the experiment in response to the variable wave climate, which included two events exceeding 2m offshore significant wave height, H_o. A single, well defined sand bar migrated seaward as the waves increased. Offshore wave conditions were generally narrowband in both frequency and direction (measured in 8m depth with a linear array of bottom mounted pressure sensors). For a more complete description of the Delilah experiment, see Birkemeier, *et al.* (1991) and Thornton and Kim (1993).

Two cases are examined in detail to contrast wave transformation over a monotonically increasing profile with a barred profile. Data to be presented are from a period when bathymetry was in a terrace-like configuration (8 October 1212 Hrs. at high tide) during which the wave field was narrowband ($f_o \approx 0.093$ Hz) with $H_o \approx 0.51$m; and during a period when the bottom was in well-developed bar-trough sequence (12 October 0718 Hrs. at low tide) with a more energetic ($H_o \approx 0.93$m) and more broadband ($0.09 < f_o < 0.12$) wave field. All spectra and bispectra are computed with 112 degrees of freedom.

IV. OBSERVATIONS

The sea surface elevation spectrum for 08 October, taken at the most offshore sensor located in about 4.5m depth (Figure 4) shows the waves were relatively narrowband (Figure 5b). Contours of bicoherence greater than the 95% significant level (b^2_{95} = 0.054 calculated as in Equation 11 for 112 d.o.f.) plotted in bi-frequency space are shown in Figure 5a. Only the unique portion of the bispectral domain is shown (Kim and Powers, 1979). The high bicoherence at the peak of the spectrum ($f_p \approx 0.093$ Hz) indicates there is significant nonlinear generation of the first harmonic (at frequency $2f_p$) by self-self interaction of the primary. The energy spectrum for 12 October (Figure 6b) is broader than the spectrum for the 8th. The nonlinear interactions are spread out over a range of incident frequencies, as shown by the bicoherence contours in Figure 6a.

The cross-shore evolution of the normalized third moment statistics (wave skewness and negative asymmetry) across the bottom profile are shown in the lower panel of Figure 7 for 08 October. The negative asymmetry is due to the selection of the positive offshore coordinate reference frame. The observed spatial distribution of the percent wave breaking is shown in the upper panel. The observed breaking region starts from about 80m offshore and increases monotonically towards the shoreline where nearly all the

waves are breaking. The skewness is high offshore and increases slightly as the narrowband waves propagate shoreward. On the other hand, the asymmetry is nearly zero offshore, but increases rapidly beyond the break point as waves shoal, suggesting the waves are pitching forward just prior to breaking (similar to results obtained by Elgar and Guza, 1985). Inside the break point, the asymmetry remains high all the way to the shoreline.

Percent breaking, skewness and asymmetry for the well-developed barred profile (12 October) are shown in Figure 8. Waves began to break about 130 meters offshore, increasing to a maximum of over 60 percent at the crest of the bar. The percentage of wave breaking decreases as waves propagate into the deeper water of trough of the bar, reaching a minimum of less than 5% at the shoreward limits of the trough and then increases again as the waves break on the foreshore.

The skewness is high offshore, increasing gradually as waves shoal, break on the bar, and reform in the trough. Only very near the shore-break does the skewness decrease. The asymmetry is small offshore (similar to the 8th) and again increases sharply just prior to breaking. The asymmetry is largest over the bar crest where the maximum percent of waves are breaking. Inside the bar crest, the asymmetry increases again at the shore-break.

The cross-shore changes in the relative amplitudes of

the primary, a_o, occurring at frequency f_p, and the first two harmonics, a_1b_1 and a_2b_2, (obtained from Figures 5a and 6a), occurring at frequencies $2f_p$ and $3f_p$, are shown in Figure 9 for 08 October (plotted as the ratios a_1b_1/a_o and a_2b_2/a_o). As the waves propagate shoreward the amplitudes of the harmonics grow relative to the primary, increasing more rapidly inside the surf zone where breaking limits the size of a_o. The bicoherences and biphases between the primary and harmonics are also shown in Figure 9. The bicoherences are strong from offshore through the surf zone showing the wave field to be significantly coupled nonlinearly. The relative phase of the harmonics to the primary (the biphase) is nearly zero offshore (in-phase) where the waves are peaked up but not pitched forward. The biphase of both harmonics increases gradually as waves approach the surf zone, continues to steepen as waves begin to break, and approaches a maximum biphase of about $-\pi/2$ in the inner surf zone.

The amplitude ratios, bicoherences, and biphases for the broader, more energetic (12 October) data are shown in Figure 10. The harmonic amplitudes are high both offshore and in the surf zone, including the trough region shoreward of the well-developed bar. The bicoherences are also high throughout the shoaling and breaking regions, except very near the shoreline. The biphases of the harmonics again increase from approximately zero offshore to near $-\pi/2$ over

the bar crest. The change toward smaller biphase of the 2nd harmonic, while its amplitude and coherence remain high, suggests significant nonlinear evolution in the trough of the bar, leading to a less pitched forward wave.

The root mean square (rms) wave face slopes calculated from the derivatives of the time series and from the maximum slope determined from the averaged waveform calculated using the bispectral coefficient (Figures 9 and 10) are shown in Figures 11 and 12. For 08 October (Figure 11), both methods show an increase in wave face angle as waves approach and then enter the surf zone. Offshore the estimates from the time series are lower than from the bispectral method, not surprising considering that time series includes all waves whereas the waveform expressed by Equation 14 includes only phase-locked harmonics and excludes other coupled wave motions. Wave slopes are maximum near the outer limits of the surf zone, and decrease slightly as wave amplitudes are reduced by breaking. The wave slope behavior for 12 October is similar to 08 October, with maximum wave slope near the bar at the outer edge of the surf zone (Figure 12).

The predicted wave slopes computed from the roller model (Equation 3) calibrated to best fit observations of percent breaking are also shown in Figures 11 and 12. The upper panels show the best fit for ψ = 4.35 and ψ = 4.05 for 08 and 12 October. The value of H_b in Equation 3 is obtained by multiplying the $H_{rms} = \sqrt{8}\,\sigma_\eta$, where σ_η is the

surface elevation variance, by the Rayleigh distribution and a spatial weighting function calibrated from percent breaking observations (Lippmann and Thornton, 1996, Equation 23). The wavelength (L) is computed from f_p and local depth using the shallow water approximation. In the surf zone the cross-shore behavior of the roller model predicted slopes is in qualitative agreement with the observed slopes. The roller model slopes are maximum in the outer limits of the surf zone, and decrease in the trough. The qualitative agreement suggests the roller model does a reasonable job of representing wave breaking in the surf zone.

V. DISCUSSION

Wave slope predictions are dependent on the value of ψ, which in turn is dependent on the accuracy of the wave and roller transformation model. This means that accurate estimates of wave energies and percent breaking distributions are vital steps in accurately predicting wave slopes. The presence of the bar tends to complicate the predictions by causing a region of intense breaking followed by a region of decreased breaking. The spatial misrepresentations in the breaking region alter the ψ value which gives the best fit to the percent breaking observations (Figures 11a and 12a). Fortunately wave heights and breaking observations are usually well modeled using the energy balance equations. Thus, differences between calculations from observations and predictions in the estimated value of ψ are minor (Lippmann and Thornton, 1996). The effects on wave slope predictions are also minor.

The LT96 roller model assumes constant ψ across the bottom profile when estimating the wave slopes. In their model, wave face slopes are a function of the local, ensemble averaged breaking wave steepness (Equation 3). The data and model estimated wave face slopes are in general qualitative agreement (particularly in the surf zone), suggesting that the wave face angles are indeed proportional to wave steepness. The changes in steepness are the result

of the cumulative effects of both the evolution of the wave profile from a skewed, Stokes-like waveform to a more pitched forward, saw-toothed like profile, and from the dissipative effects of wave breaking which severely limit wave heights, but not wavelengths, in the surf zone.

The roller model predicts the wave face slope of breaking waves only, whereas the time series measurements include all waves, breaking and non-breaking. The bispectral waveform describes only the shape of the primary waveform, and thus should be better representative of the breaking waves wave slopes. Therefore, outside the surf zone, model and bispectral measured wave slopes are expected to be greater than the averaged wave face slopes from all waves of the time series (Figures 11b and 12b). Inside the surf zone where most of the waves are breaking, the roller model predictions are in good qualitative agreement with the root mean square (rms) averaged wave face slopes. The wave face slope comparisons are reasonable for both narrowband waves over a monotonically increasing bathymetry and the more complicated shoaling and breaking over a barred beach.

Both measured and roller modeled wave face slopes (Figures 11b and 12b), which range about 4-10 degrees (6 degrees is about a 1:10 slope for comparison), seem small compared with casual observations of breaking waves which appear to approach vertical for plunging breakers. The very steep wave faces observed on large breakers are horizontally

small in dimension compared with the wavelength. Thus sampling the very narrow, highly nonlinear wave crest is important, and has proved limiting using standard wave measuring techniques (i.e., bottom pressure meters), which depend on the sensor resolution and sampling rates (typically 2-8 Hz for surf zone applications). Even at much higher rates it is still not clear that local time series are adequate, owing to hydrodynamic filtering of the very high frequencies (which are attenuated even in shallow water) that produce the steepness in the upper crest of the wave.

Direct measurements of wave slopes in the crest of the wave requires spatially resolving measurement techniques, which owing to logistical difficulties in deploying a large array of fixed instruments, will most likely have to have a remote sensing nature (such as stereo video). The direct spatial measurements also eliminate the need to estimate the local phase speed necessary when using single point time series (Equation 13).

Ensemble averaged phase speeds in shallow water are modeled with linear theory (Thornton and Guza, 1982; Lippmann and Holman, 1991; and others), which tend to underestimate actual phase speeds due to some amplitude dispersion. Underestimation of phase speed results in overestimating the wave face slope magnitude using Equation 13. Including amplitude dispersion would greatly complicate

the analysis. The linear approximation, however, is sufficient for observing qualitative wave face slope changes.

Wave face slopes change as a result of evolution of skewness, asymmetry, and wave steepness, which in turn are determined by the shoaling topography (Figures 11c and 12c) and wave breaking distributions, which may be highly variable in the surf zone. Observations of wave asymmetries and percent breaking (Figures 7b and 8b) appear to have similar spatial distributions (Figures 7a and 8a). Even though wave breaking is expected to significantly modify the wave steepness, the exact effect on wave skewness and asymmetries can not be resolved.

Bispectral analysis leads to estimates of wave slopes through estimates of harmonic amplitudes (Figures 9b and 10b), and the degree of coupling between waves and their phase relationships (Figures 9c and 10c) at interacting frequencies. Estimates of these quantities can be sensitive to the method of computing the bispectrum (Elgar and Guza, 1988). In this work, the filtered time series are broken up into 512 point samples (corresponding to 256 second records), a Hanning data window applied, and then are averaged with no frequency merging done. The effects of frequency bandwidth on wave slope calculations derived from bispectral estimates was tested by using a range of ensemble widths from 256 to 2048 points (corresponding to 448 to 56 degrees

of freedom). The resulting deviation in wave slope was slight, with qualitative trends across-shore being preserved, and about a ±0.5-1.0 degree variation occurring occasionally about an average wave slope which was not substantially effected. Varying the high (and low) frequency cutoff's from the band-pass filtered applied to the raw time series did not affect our estimate of slope in any of our methods.

VI. CONCLUSIONS

Ensemble averaged wave face slopes of breaking waves in the surf zone are calculated directly from the time series and from an averaged waveform calculated from bispectral coefficients and compared with predictions from a wave transformation model that includes wave breaking described by rollers. Also examined is the relationship between percent breaking and both normalized third moments (skewness and asymmetry) and bispectral statistics.

The nonlinear evolution of waveform across the breaking region is qualitatively described from observations of third moment statistics and from examination of the phase relationships between the primary frequency and its coupled harmonic components. The roller model predictions are in qualitative agreement with the observed waveform calculated from observations.

The skewness is generally high across the shoaling and breaking regions, consistent with a peaked waveform common to Stoke-like gravity waves. As the waves approach breaking, the wave crests become more pitched forward, transforming from near zero asymmetry offshore (indicating little or no pitch) to a maximum in the inner surf zone (indicating a more pitched forward waveform). The asymmetry reaches a maximum coincident with the location of breaking. Bispectral analysis shows that coupled harmonic amplitudes

grow through the shoaling and breaking regions relative to the amplitude of the primary incident frequency. Shoreward of a well-developed bar, the waves gradually reform from breaking pitched forward bores to skewed non-breaking waves. It is not clear that this transition is due to topographical influence or wave breaking distributions, or both to some degree.

For the barred profile the average wave face angle first increases as waves pitch forward over the bar just prior to breaking, then decreases as waves propagate into the trough, and then increases again as waves break at the shoreline. The wave slopes predicted from a calibrated (with percent breaking observations) roller transformation model are in qualitative agreement with the wave slope observations, suggesting that roller theory well represents waveform evolution particularly in the breaking region.

APPENDIX

Figure 1. Roller model predictions of percent wave breaking from video recordings of the surf zone from 10 October, 1990 during the Delilah experiment (From Lippmann and Thornton, 1996). The upper panel shows percent breakers observed in the field (circles) and predicted by the roller model (solid line) on the nearshore profile shown in the lower panel. Also shown for comparison are predictions from a (typical) previous wave transformation model (dashed line, Lippmann, *et al.*, 1996).

Figure 2. Schematic showing geometry for a wave with turbulent roller on the linear wave face (modified slightly from Lippmann and Thornton, 1996). Variables are defined in the text.

Figure 3. Schematic (modified from Doering, 1988) showing sinusoidal (horizontal and vertical symmetry), skewed (horizontal symmetry; vertical asymmetry) and asymmetric (horizontal asymmetry; vertical symmetry) waveforms. Amplitude and phase relationships relative to the primary frequency are also shown to the right of each wave profile. Note that although the amplitude spectra are identical for the skewed and asymmetric waves, the harmonics for the skewed wave are in-phase, whereas the harmonics are $\pi/2$ phase shifted relative to the primary for the asymmetric

wave. Phase relationships between primary and harmonics which are between 0 and $\pi/2$ have both skewed and asymmetric characteristics.

Figure 4. Beach profiles for 08 and 12 October during the Delilah experiment and the location of pressure sensors. Cross-shore distance is relative to the Field Research Facility (FRF) coordinate system and depths are relative to National Geodetic Vertical Datum (NGVD).

Figure 5. (a) Sea surface elevation energy-density spectrum for 08 October at 1212 Hrs. observed at the most seaward sensor (Figure 4). Spectrum is computed from one hour time series with 56 d.o.f. corresponding to a frequency bandwidth of 0.0075 Hz. (b) Contours of significant bicoherence (greater than the 95% significant level of 0.23) plotted in bi-frequency space corresponding to the energy-density spectrum in (a). Contour interval is 0.1 with maximum bicoherence of 0.79 occurring at $f_1 = f_2 = 0.094$ Hz.

Figure 6. (a) Same as Figure 5a for 12 October at 0718 hrs. (b) Same as 5b with maximum bicoherence of 0.48 occurring at $f_1 = 0.094$ Hz and $f_2 = 0.125$ Hz.

Figure 7. Cross-shore evolution of the normalized third moments skewness and negative asymmetry (center panel) for 08 October. Statistics are computed in the time domain from

bandpass filtered sea surface elevation time series. The bathymetry is shown in the lower panel and the observed percent wave breaking in the upper panel for comparison.

Figure 8. Same as Figure 7 for 12 October at 0718 hrs.

Figure 9. Cross-shore evolution of (b) observed ratio of primary to first (Stars) and second (circles) harmonic amplitudes, (c) negative biphase between primary and first (stars) and second (circles) harmonics, and (d) bicoherence between interacting primary frequencies (stars) and interactions between primary and harmonic frequencies (circles) for 08 October. The bathymetry is shown in (e), and the observed percent breaking in (a) for comparison.

Figure 10. Same as Figure 9 for 12 October.

Figure 11. Cross-shore evolution in rms wave face slopes (middle panel) calculated from the time series and maximum slope from nonlinearly coupled Equation 14 for 08 October. Observed (stars) and roller model predicted (solid line) percent breaking is shown in the upper panel. The roller model is from Lippmann and Thornton (1996) and has best fit ψ parameter if 4.35. Also shown in the middle panel is the roller model generated wave slopes based on the ψ value obtained (Equation 3). The bathymetry is shown in the lower

panel for reference.

Figure 12. Same as Figure 11 for 12 October. Best fit ψ value from roller modeling is 4.05.

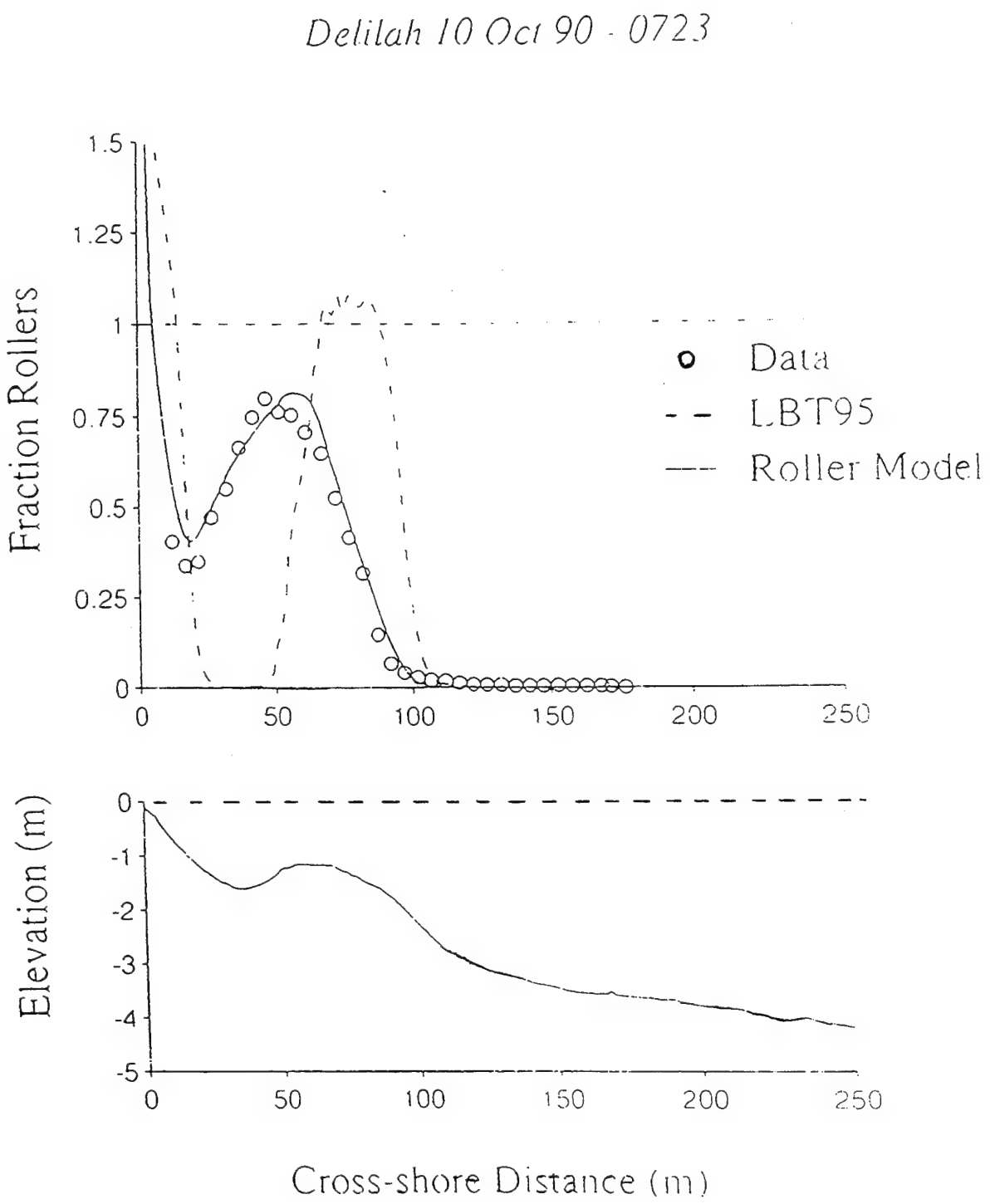
Delilah 10 Oct 90 - 0723
Fraction Rollers
1.5
1.25
1
0.75
0.5
0.25
0
0
50
100
150
200
250
Data
LBT95
Roller Model
Elevation (m)
0
-1
-2
-3
-4
-5
0
50
100
150
200
250
Cross-shore Distance (m)

Figure 1.

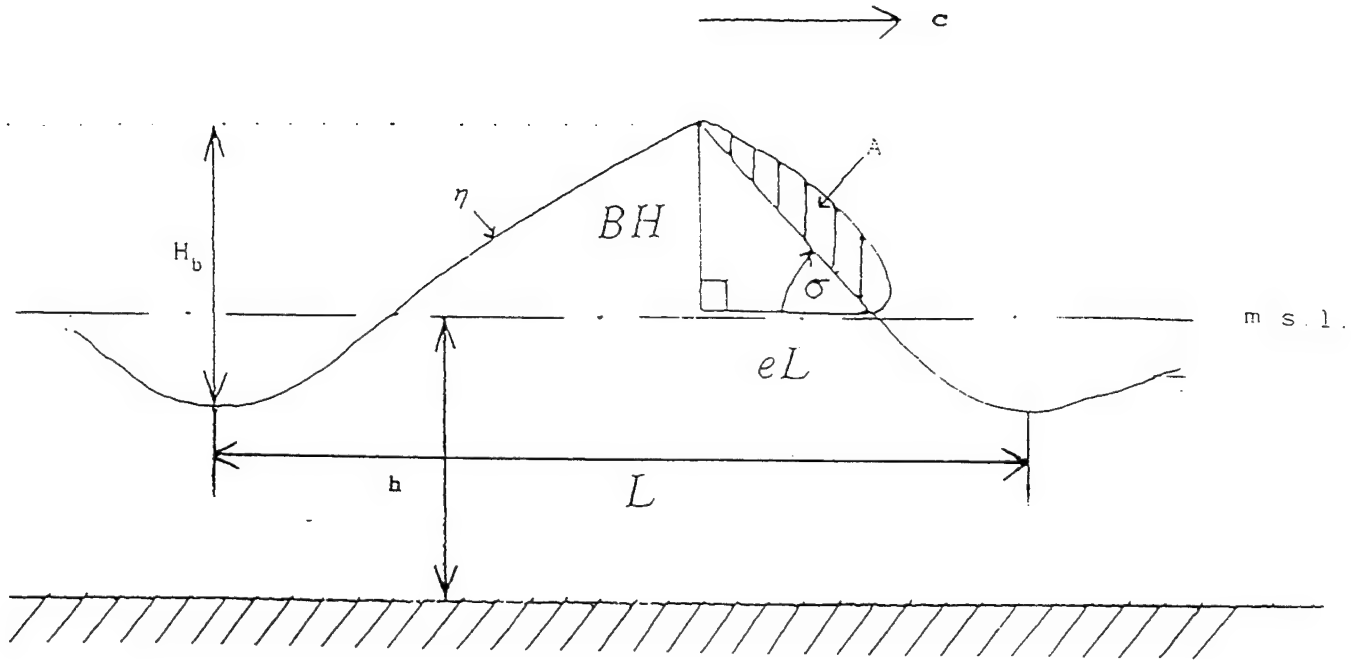

Figure 2.

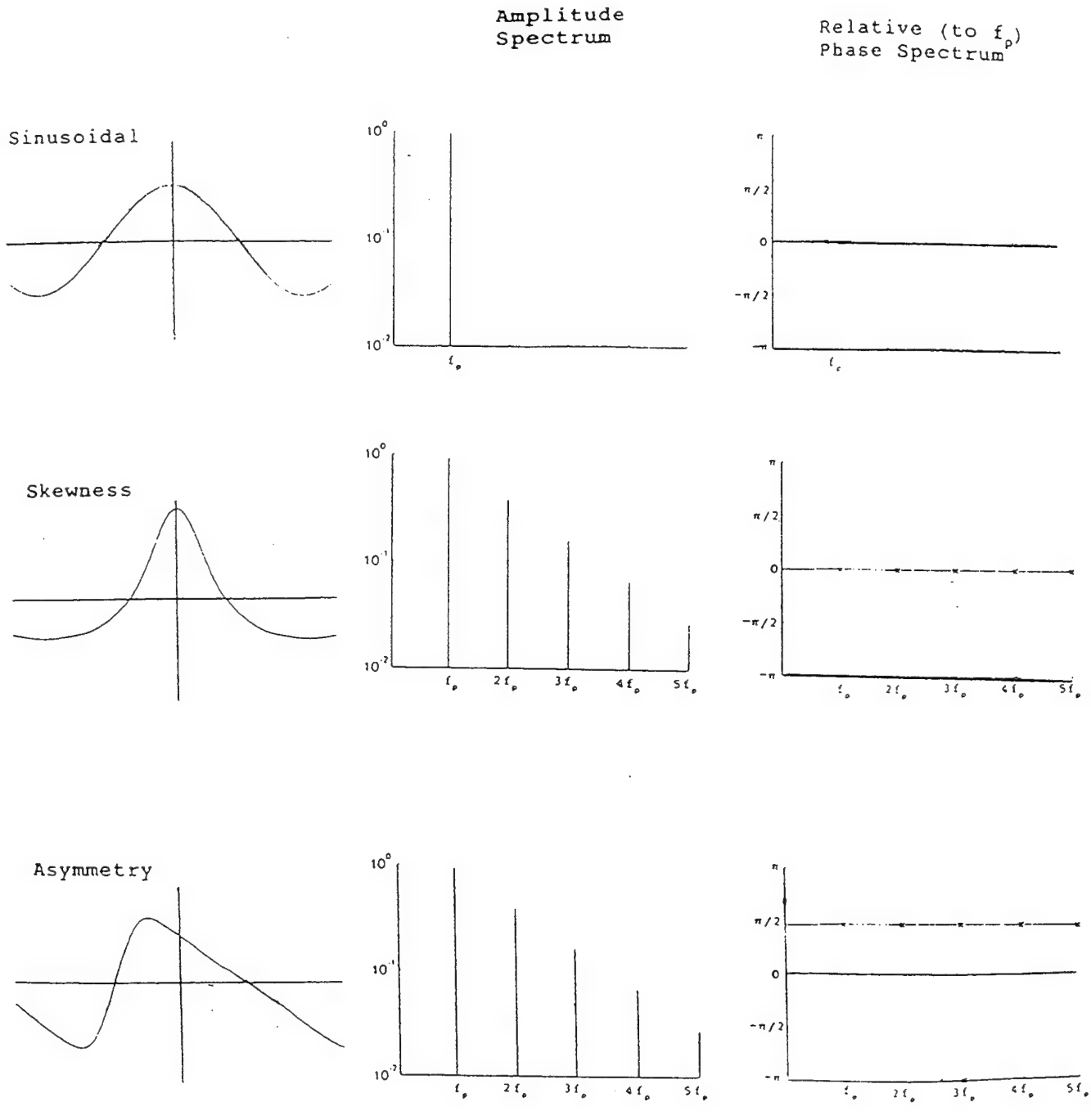
Amplitude Spectrum
Relative (to f_p) Phase Spectrum
Sinusoidal
Skewness
Asymmetry
10^0
10^{-1}
10^{-2}
π
$\pi/2$
0
$-\pi/2$
$-\pi$
f_p
$2f_p$
$3f_p$
$4f_p$
$5f_p$

Figure 3.

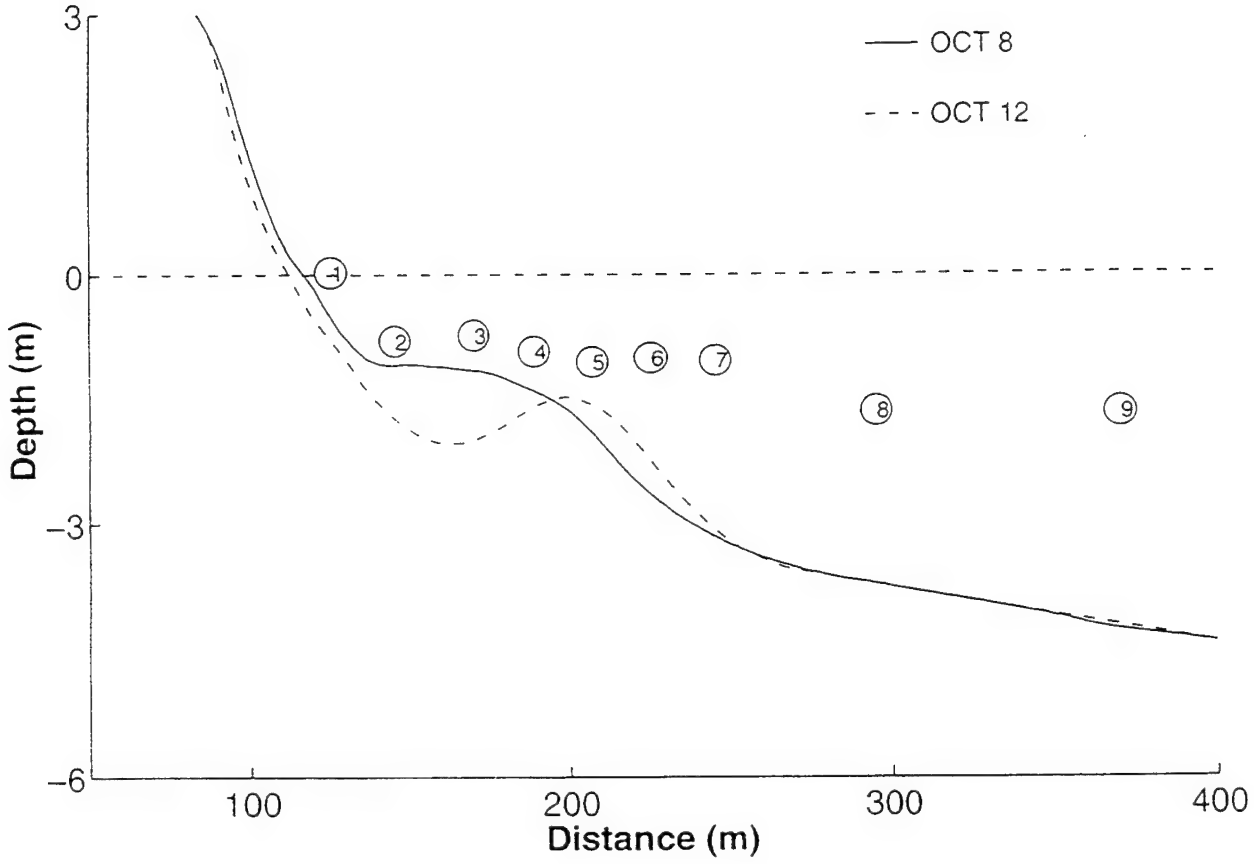

Figure 4.

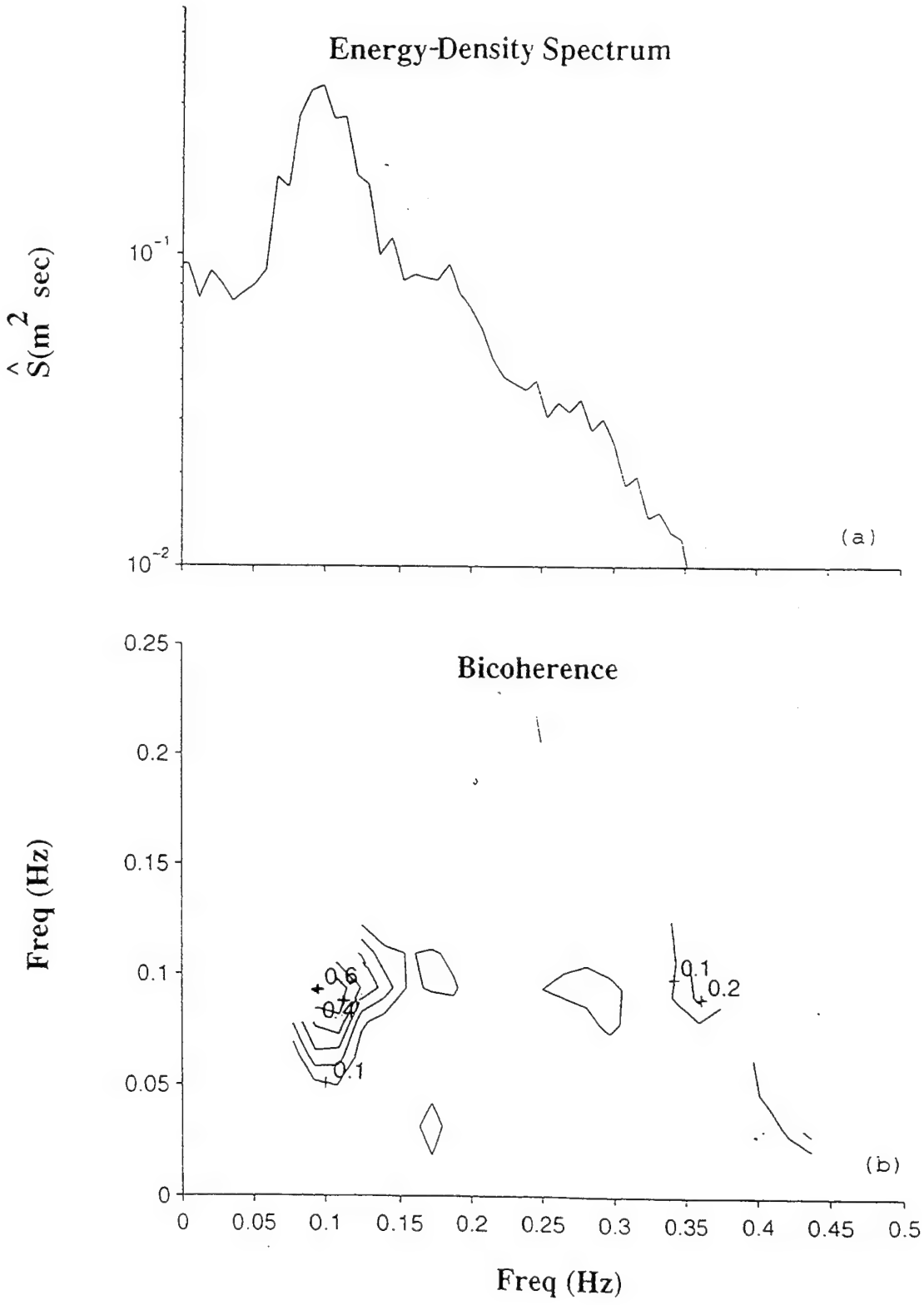
08 October 1212 Hrs.
Energy-Density Spectrum
$\hat{S}(m^2 sec)$
10^{-1}
10^{-2}
(a)
Bicoherence
Freq (Hz)
0.25
0.2
0.15
0.1
0.05
0
0.6
0.4
0.1
0.1
0.2
0 0.05 0.1 0.15 0.2 0.25 0.3 0.35 0.4 0.45 0.5
Freq (Hz)
(b)

Figure 5.

12 October 0718 Hrs.

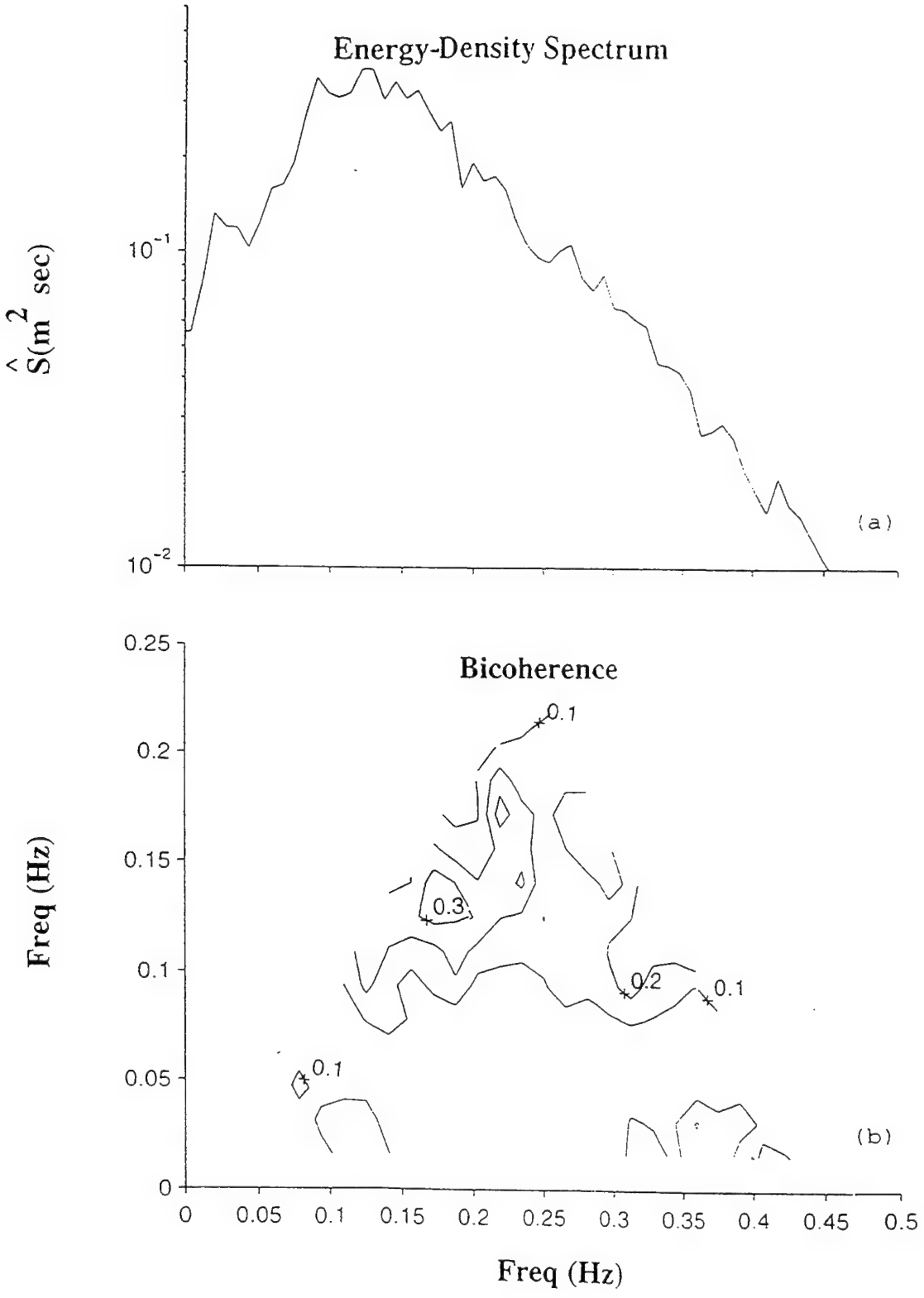

Figure 6.

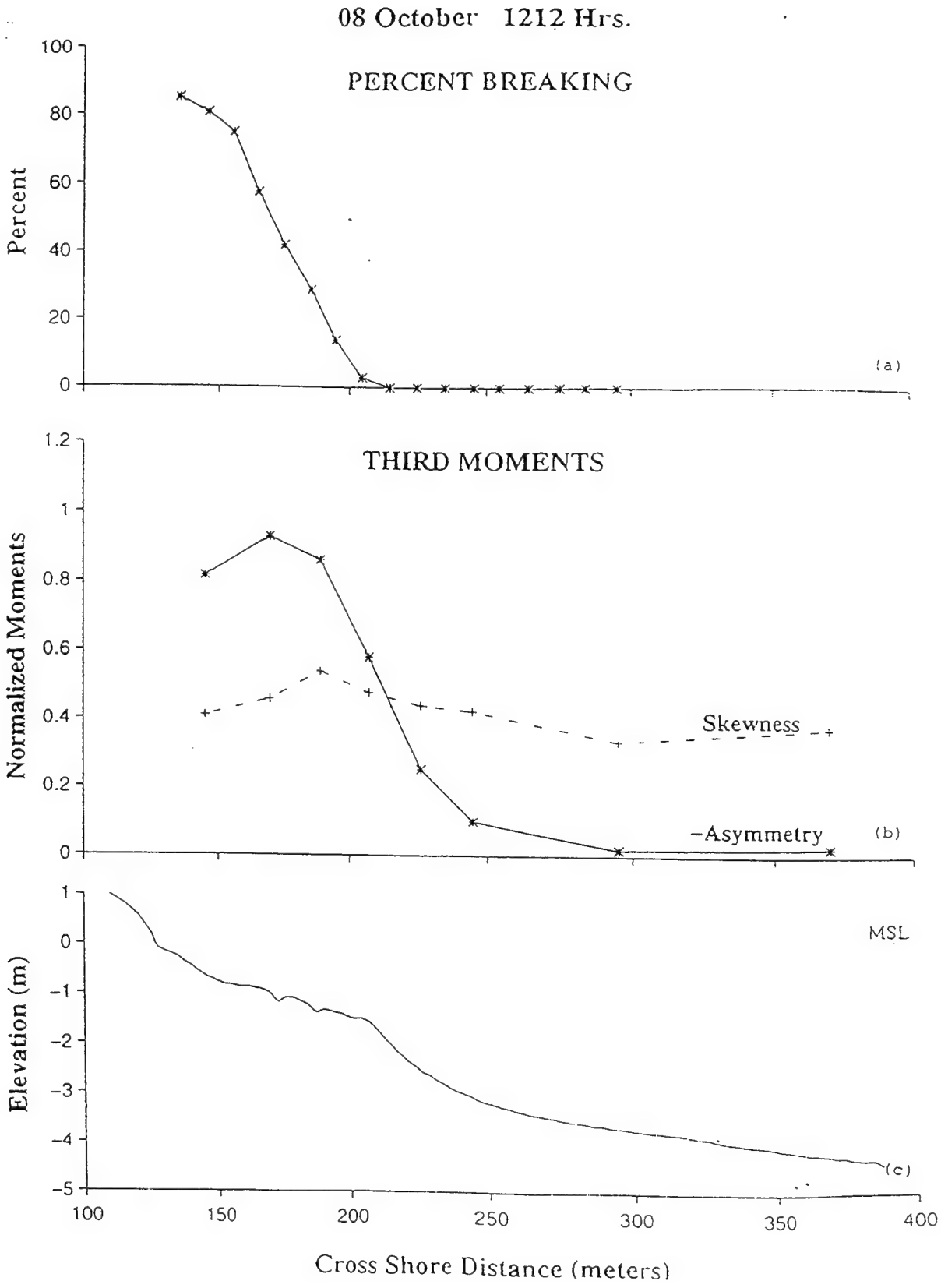
08 October 1212 Hrs.
PERCENT BREAKING
Percent
100
80
60
40
20
0
(a)
THIRD MOMENTS
Normalized Moments
1.2
1
0.8
0.6
0.4
0.2
0
Skewness
Asymmetry
(b)
Elevation (m)
1
0
-1
-2
-3
-4
-5
MSL
(c)
100
150
200
250
300
350
400
Cross Shore Distance (meters)

Figure 7.

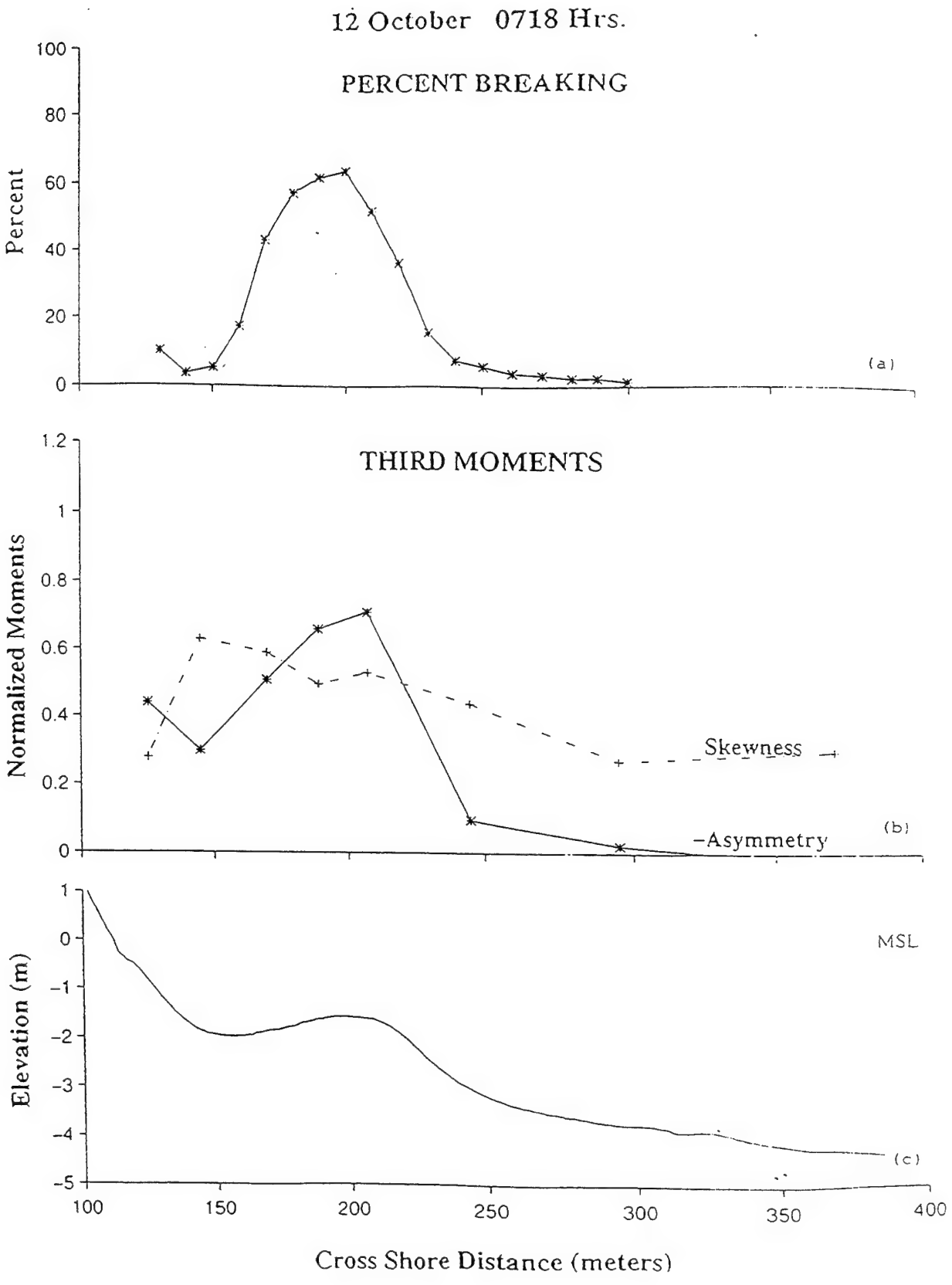
12 October 0718 Hrs.
PERCENT BREAKING
Percent
100
80
60
40
20
0
(a)
THIRD MOMENTS
Normalized Moments
1.2
1
0.8
0.6
0.4
0.2
0
Skewness
Asymmetry
(b)
Elevation (m)
1
0
-1
-2
-3
-4
-5
MSL
(c)
100
150
200
250
300
350
400
Cross Shore Distance (meters)

Figure 8.

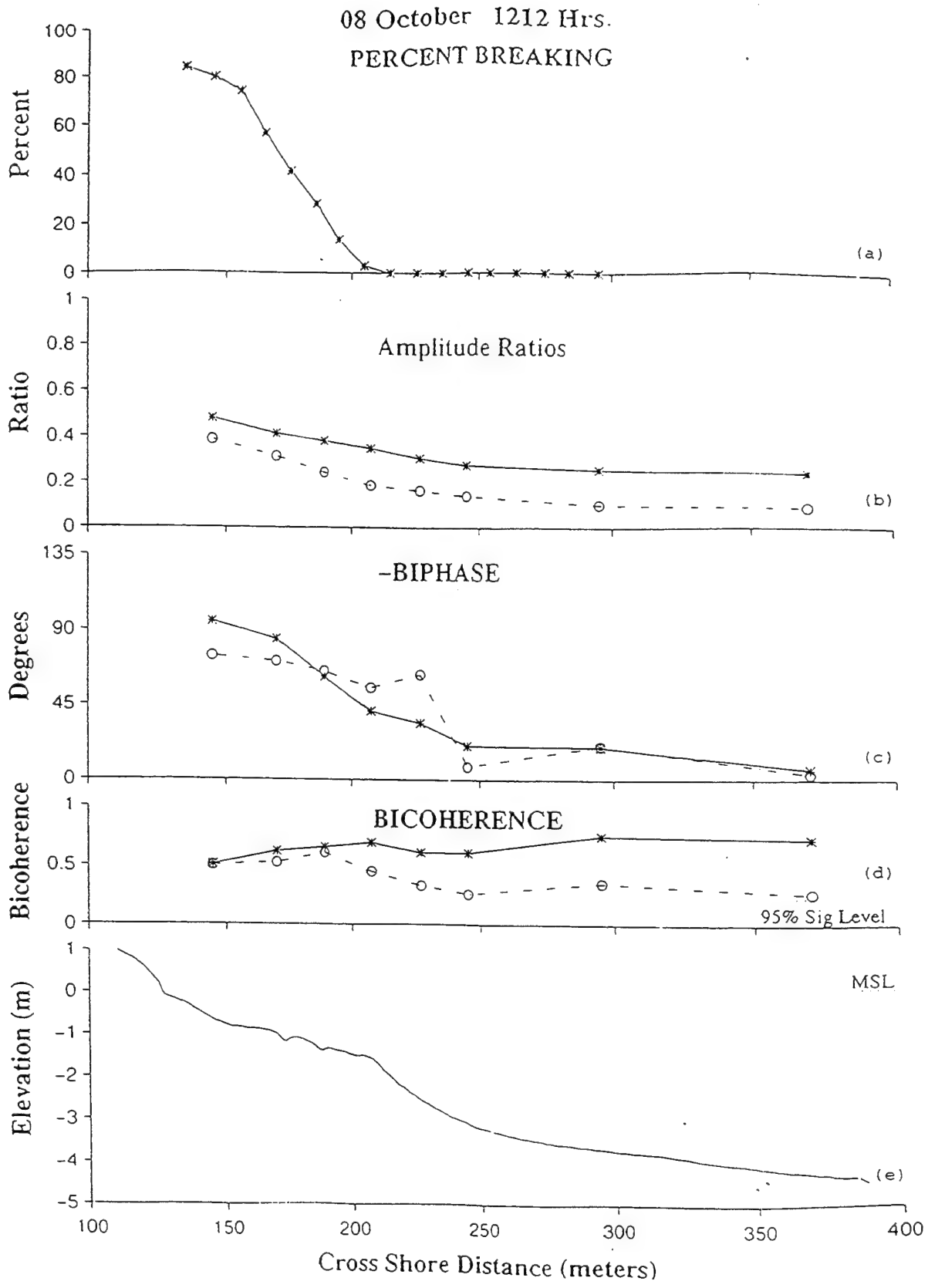
08 October 1212 Hrs.
PERCENT BREAKING
Percent
100
80
60
40
20
0
(a)
Amplitude Ratios
Ratio
1
0.8
0.6
0.4
0.2
0
(b)
-BIPHASE
Degrees
135
90
45
0
(c)
BICOHERENCE
Bicoherence
1
0.5
0
(d)
95% Sig Level
MSL
Elevation (m)
1
0
-1
-2
-3
-4
-5
(e)
100
150
200
250
300
350
400
Cross Shore Distance (meters)

Figure 9.

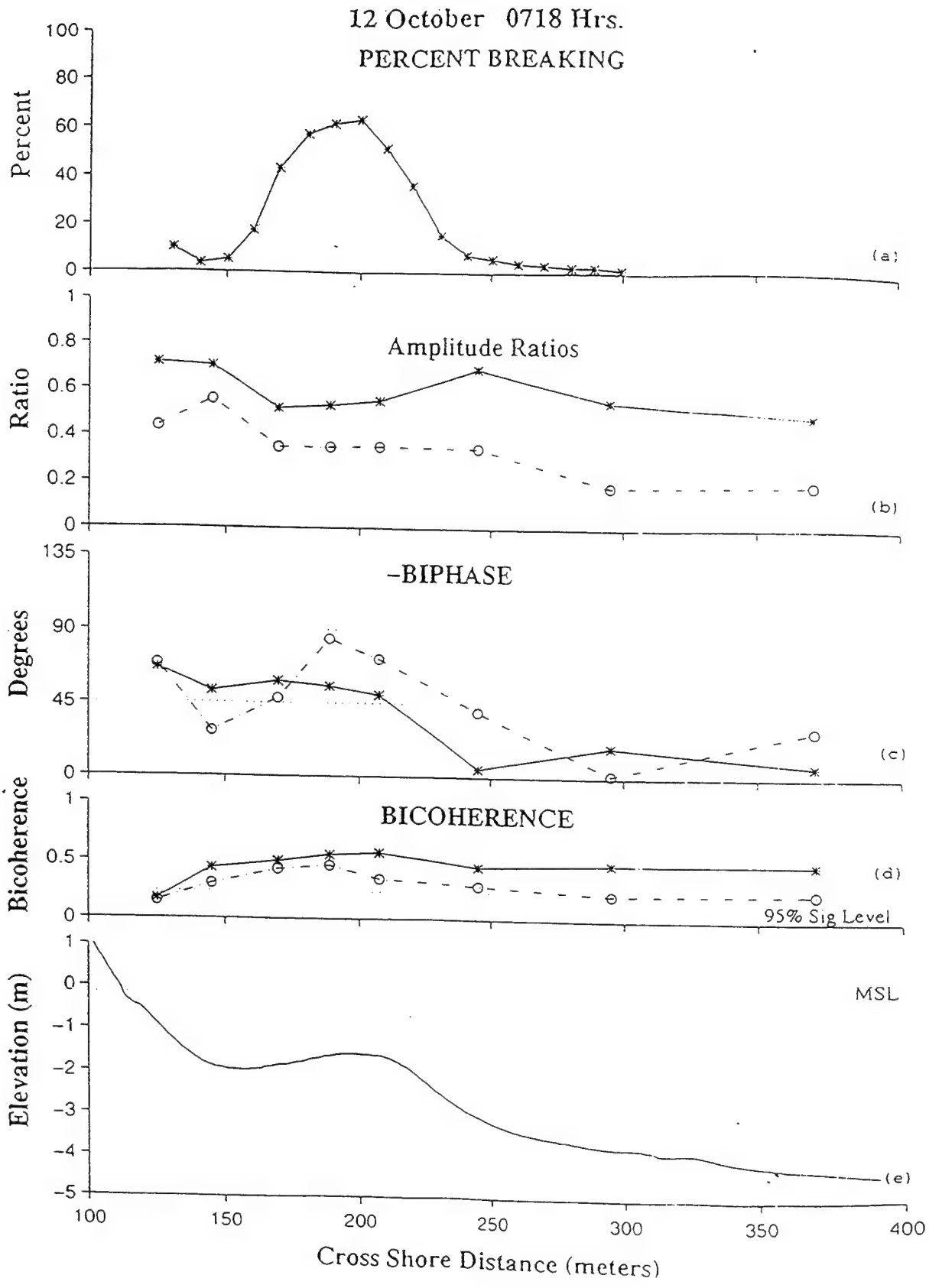
12 October 0718 Hrs.
PERCENT BREAKING
Percent
100
80
60
40
20
0
(a)
Amplitude Ratios
Ratio
1
0.8
0.6
0.4
0.2
0
(b)
-BIPHASE
Degrees
135
90
45
0
(c)
BICOHERENCE
Bicoherence
1
0.5
0
(d)
95% Sig Level
MSL
Elevation (m)
1
0
-1
-2
-3
-4
-5
(e)
100
150
200
250
300
350
400
Cross Shore Distance (meters)

Figure 10.

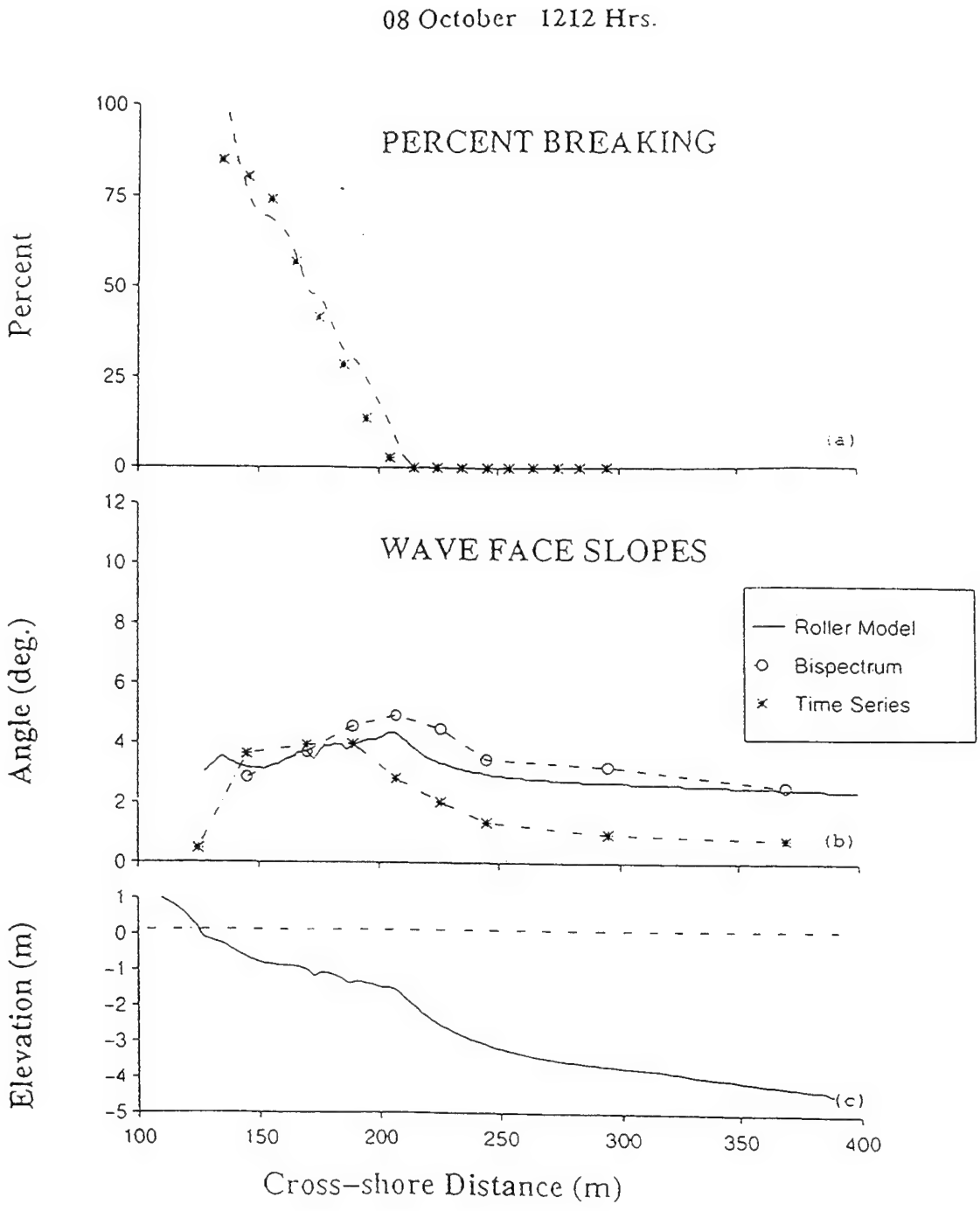
08 October 1212 Hrs.
PERCENT BREAKING
Percent
100
75
50
25
0
(a)
WAVE FACE SLOPES
Angle (deg.)
12
10
8
6
4
2
0
Roller Model
Bispectrum
Time Series
(b)
Elevation (m)
1
0
-1
-2
-3
-4
-5
(c)
100
150
200
250
300
350
400
Cross-shore Distance (m)

Figure 11.

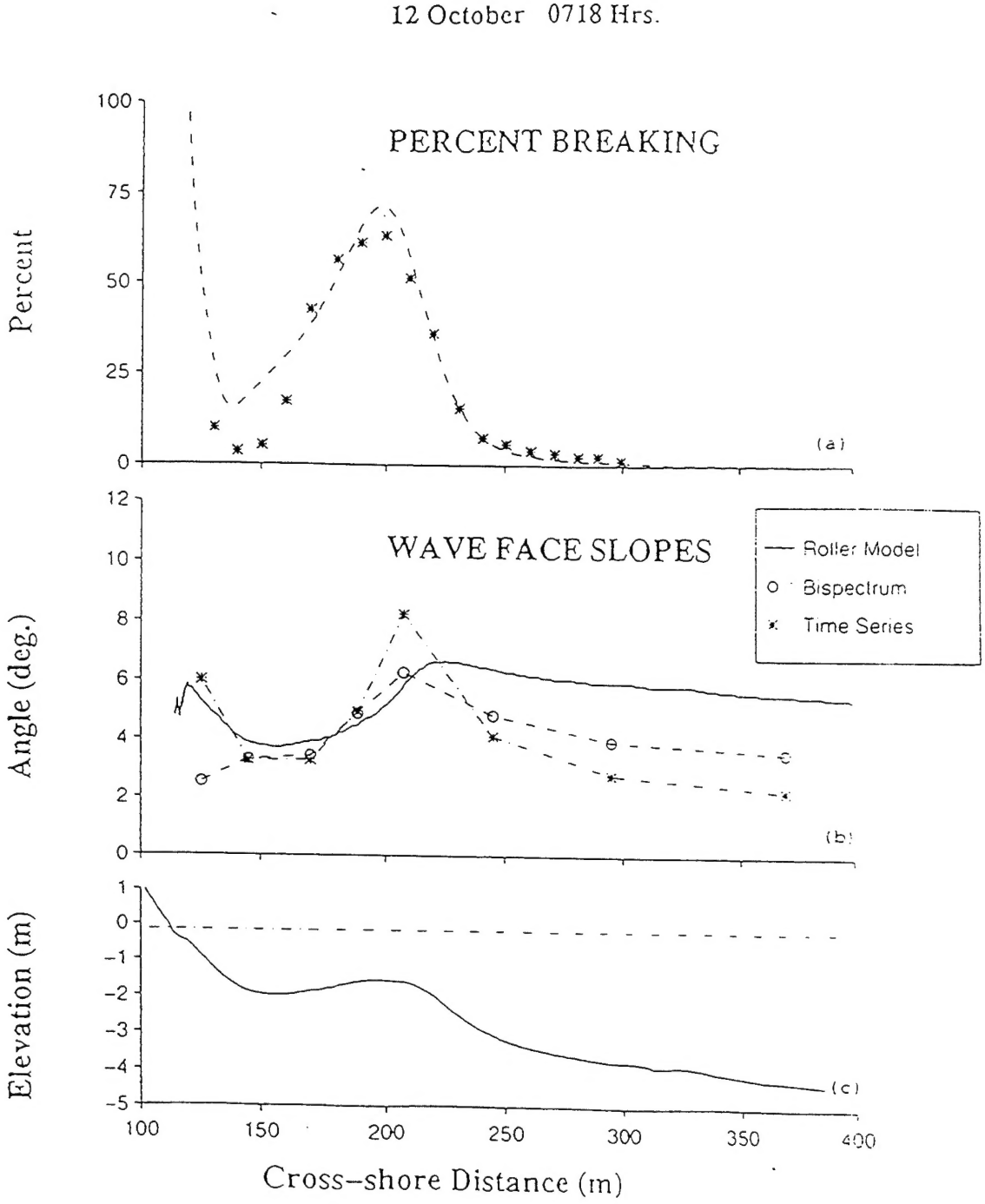
12 October 0718 Hrs.
PERCENT BREAKING
Percent
100
75
50
25
0
(a)
WAVE FACE SLOPES
Roller Model
Bispectrum
Time Series
Angle (deg.)
12
10
8
6
4
2
0
(b)
Elevation (m)
1
0
-1
-2
-3
-4
-5
(c)
100
150
200
250
300
350
400
Cross-shore Distance (m)

Figure 12.

REFERENCES

Battjes, J. A., and J. P. F. M. Janssen, 1978, Energy loss and set-up due to breaking of random waves, in *Proc. 16th International Conf. Coast. Eng.*, ASCE, New York, 569-587.

Bendat, J. S. and A. G. Piersol, 1986, *Random Data: Analysis and Measurement Procedures*, John Wiley & Sons, Inc., 484-514.

Birkemeier, W. A., and C. Mason, 1984, The CRAB: A unique nearshore surveying vehicle, *J. Surv. Eng.*, 110(1), 1-7.

Birkemeier, W. A., K. K. Hathaway, J. M. Smith, C. F. Baron, and M. W. Leffler, 1991, *Delilah Experiment: Investigator's Summary Report*, Department of the Army, US Army Corps of Engineers.

Dally, W. R., and C. A. Brown, 1995, A modeling investigation of the breaking wave roller with application to cross-shore currents, *J. Geophys. Res.*, 100(C12), 24873-24883.

Deigaard, R., 1993, A note on the three-dimensional shear stress distribution in a surf zone, *Coast. Eng.*, 20, 157-171.

Doering, J. R. C., 1988, *Wave-Wave Interactions In The Nearshore*, Ph. D. Thesis, Dalhousie University, pp. 139.

Duncan, J. H., 1981, An experimental investigation of breaking waves produced by a towed hydrofoil, *Proc. R. Soc. Lond.*, A377, 331-348.

Elgar, S. and R. T. Guza, 1985, Observations of bispectra of shoaling surface gravity waves, *J. Fluid Mech.*, 161, 425-448.

Elgar, S. and R. T. Guza, 1988, Statistics of bicoherence, *IEEE Trans. of Acoustics, Speech, and Signal Processing*, 36(10), 1667-1668.

Engelund, F., 1981, A simple theory of weak hydraulic jumps, *Progress Report No. 54*, Inst. of Hydrodynamics and Hydraulic Engineering, ISVA, Tech. Univ. Denmark, 29-32.

Guza, R. T. and E. B. Thornton, 1980, Local and shoaled comparisons of sea surface elevations, pressures, and velocities, *J. Geophys Res.*, 85(C3), 1524-1530.

Hasselman, K., W. Munk, and G. MacDonald, 1963, Bispectra of ocean waves in *Time Series Analysis* (Edited by M. Rosenblatt), 125-139.

Kim, Y. C. and E. J. Powers, 1979, Digital bispectral analysis and its applications to non-linear wave interactions. *IEEE Trans. on Plasma Sc.*, 1, 120-131.

LeMehaute, B., 1962, On non-saturated breakers and the wave run-up, *in Proceedings 8th International Conf. Coast. Eng.*, ASCE, New York, 77-92.

Lippmann, T. C. and R. A. Holman, 1991, Phase speed and angle of breaking waves measured with video techniques, *Proceedings Coast. Sediments '91 Specialty Conf.*, ASCE, New York, 542-556.

Lippmann, T. C. and E. B. Thornton, 1996, The spatial distribution of wave rollers on a barred beach, in press.

Lippmann, T. C., A. H. Brookins, and E. B. Thornton, 1996, Wave energy transformation on natural profiles, in press.

Nairn, R. B., J. A. Roelvink, and H. N. Southgate, 1990, Transition zone width and implications for modelling surf zone hydrodynamics, *in Proceedings 22nd International Conf. Coast. Eng.*, ASCE, New York, 68-81.

Roelvink, J. A., 1993, Dissipation in random wave groups incident on a beach, *Coast. Eng.* 19, 127-150.

Svendsen, I. A., 1984, Wave heights and set-up in a surf zone, *Coast. Eng.*, 8, 303-329.

Thornton, E. B. and R. T. Guza, 1982, Energy saturation and phase speeds measured on a natural beach, *J. Geophys Res.*, 87, 9,499-9,508.

Thornton, E. B. and R. T. Guza, 1983, Transformation of wave height distribution, *J. Geophys Res.*, 88, 5,925-5,938.

Thornton, E. B. and C. S. Kim, 1993, Longshore current and wave height modulation at tidal frequency inside the surf zone, *J. Geophys Res.*, 98, 16,509-16,519.

INITIAL DISTRIBUTION LIST

1. Defense Technical Information Center.....2
   8725 John J. Kingman Road, STE 0944
   Fort Belvoir, Virginia 22060-6218

2. Dudley Knox Library.....2
   Naval Postgraduate School
   411 Dyer Road
   Monterey, California 93943-5101

3. E. B. Thornton, Code OC/Tm.....1
   Naval Postgraduate School
   Monterey, California 93943-5002

4. T. C. Lippmann.....2
   Center for Coastal Studies
   Scripps Institute of Oceanography
   University of California San Diego
   9500 Gillman Drive
   La Jolla, California 92093-0209

5. C. F. Jorgensen.....3
   37 Harrowgate Dr.
   Cherry Hill, New Jersey 08003

6. T. H. C. Herbers, Code OC/He.....1
   Naval Postgraduate School
   Monterey, California 93943-5002

7. J. H. Wilson, Code OC/Wi.....1
   Naval Postgraduate School
   Monterey, California 93943-5002

8. T. Kinder.....1
   Coastal Sciences (Code 1121CS)
   800 North Quincy Street
   Arlington, Virginia 22217

9. D. Foster.....1
   COAS, Building #104
   Oregon State University
   Corvallis, Oregon 97331